

2.9 Nonuniform potential vorticity.

Our discussion of semigeostrophic models has largely been restricted to flows with uniform potential vorticity. The only waves supported by such flows are the two Kelvin waves, or their frontal relatives. As noted in Section 2.1, the introduction of a potential vorticity gradient gives rise to a new restoring mechanism and a new class of waves which are nondispersive at long wave lengths. We discussed the case of topographic Rossby waves in a channel with a constant bottom slope $\partial h^* / \partial x^* = -s$ and a rigid upper boundary. The dispersion relation (2.1.30) governing long waves propagating on a background state of rest can be generalized to include a uniform background velocity V , in which case the wave speed becomes

$$c^* = V + \left(\frac{dq^*}{dx^*} \right) \frac{w^{*3}}{n^2 \pi^2}, \quad n = 1, 2, 3, \dots \quad (2.9.1)$$

where $\frac{dq^*}{dx^*} = -\frac{sf}{D^2}$. For positive s , $\partial q^* / \partial x^* < 0$ and higher potential vorticity is found on the left-hand side (facing positive y^*) of the channel. In this case the propagation tendency of the waves is against the background flow and hydraulic criticality ($c^*=0$) occurs when

$$V = \frac{sfw^{*3}}{D^2 n^2 \pi^2}. \quad (2.9.2)$$

In the opposite case ($\partial q^* / \partial x^* > 0$), all waves propagate towards positive y^* . Critical flow for this example therefore requires that the potential vorticity increase to the left of the flow direction.

The presence of a potential vorticity gradient in combination with a free surface or interface leads to analytical difficulties in connection with the cross-stream structure equation (2.1.14). The difficulty can be described by first noting the connection between ψ and d implied by the geostrophic relation:

$$\frac{\partial \psi}{\partial x} = vd = \frac{1}{2} \frac{\partial d^2}{\partial x} + d \frac{\partial h}{\partial x} \quad (2.9.3)$$

If $\partial h / \partial x = 0$ integration of this equation from the channel side wall at $x=w/2$ to a point in the interior yields

$$\psi = 1 + \frac{1}{2}(d^2 - d^2(\frac{1}{2}w, y)) \quad (2.9.4)$$

where $\psi=1$ has been imposed at $y=w/2$. Equation (2.1.14) may now be written as

$$\frac{\partial^2 d}{\partial x^2} - q[1 - \frac{1}{2}(d^2 - d^2(\frac{1}{2}w, y))]d = -1 \quad (2.9.5).$$

If q is constant (2.9.5) reduces to the familiar linear equations that forms the basis for models considered earlier. However, a nontrivial dependence of q on ψ produces a nontrivial equation.

Some progress can be made without actually solving the particulars of the cross-stream structure. For example, Stern (1974) derives a generalized critical condition with no restriction on potential vorticity and with the requirements that the channel cross-section be rectangular ($\partial h / \partial x = 0$) and that the flow be unidirectional. A version of the proof, grounded in Stern's approach but simpler than his original proof, begins with the relation

$$v = \pm 2^{1/2} [B(1 + \frac{1}{2}(d^2 - d^2(\frac{1}{2}w, y))) - d - h]^{1/2}$$

which follows from the definition of the Bernoulli function $B(\psi)$ and from (2.9.4). Assume that the velocity is positive, so that the '+' sign is appropriate. If this v is substituted into the geostrophic relation, essentially $\partial d / v = \partial x$, and the result integrated across the channel width, one obtains

$$I_1(d_{-w/2}; w; Q) = \int_{d(\frac{1}{2}w, y)}^{(2Q+d^2(\frac{1}{2}w, y))^{1/2}} \frac{\partial d}{2^{1/2} [B(1 + \frac{1}{2}(d^2 - d_{-w/2}^2)) - d]} = w$$

The use of d as an integration variable assumes a one-to-one correspondence between x and d , and this is guaranteed when v remains positive for $-w/2 \leq x \leq w/2$. The upper limit of integration is the right wall depth $(2Q + d^2(\frac{1}{2}w, y))$ expressed in terms of the flow rate and the left wall depth. If $B(\psi)$ is known in advance, then $\mathcal{G} = I_1 - 2^{1/2}w$ can be regarded as a hydraulic functional, expressing a relationship between the single dependent variable $d(\frac{1}{2}w, y)$, the geometric variables w and h , and the parameter Q . A critical condition can thus be obtained by taking $\partial \mathcal{G} / \partial d(\frac{1}{2}w, y) = 0$ (or simply $\partial I_1 / \partial d^2(\frac{1}{2}w, y) = 0$). After use of Leibnitz's Rule and some careful integration by parts, one obtains the result

$$\int_{d(\frac{1}{2}w, y)}^{(2Q+d^2(\frac{1}{2}w, y))^{1/2}} \left(\frac{1}{dv_+^3} - \frac{1}{d^2 v_+} \right) \partial d = 0$$

Changing the integration variable from d to x (using $\partial d = v \partial x$) leads to Stern's result, which can be written in dimensional form as

$$\int_{-w^*/2}^{w^*/2} \frac{1}{v^{*2} d^*} \left(1 - \frac{v^{*2}}{gd^*} \right) \partial d^* = 0 \quad (2.9.6)$$

In essence, the local value of $v^* / \sqrt{gd^*}$ must =1 for some x^* across the channel in order for the flow to be critical. It is remarkable that this result does not depend on the Coriolis parameter f . It is also interesting that (2.9.6) appears to apply to potential vorticity waves as well as Kelvin and frontal waves. However, the restriction to unidirectional velocity profiles may disallow certain types of critical states, an issue that we will return to.

Stern's result can be used to define a type of generalized Froude number

$$F_d = \frac{\int_{-w^*/2}^{w^*/2} \frac{1}{gd^{*2}} \partial x^*}{\int_{-w^*/2}^{w^*/2} \frac{1}{d^* v^{*2}} \partial x^*} \quad (2.9.7)$$

having the property that $F_d=1$ for critical flow and $F_d \rightarrow 0$ as $v_+ \rightarrow 0$. The latter limit implies that $F_d < 1$ subcritical flow, but one should exercise caution in making this interpretation. Flows with nonuniform potential vorticity may admit to many wave modes and a particular value of F_d does not, in itself, indicate supercritical or subcritical conditions with respect to any particular wave. We only know that $F_d=1$ indicates that one of the waves is arrested.

A detailed example of hydraulic effects in the presence of both gravitational and potential vorticity dynamics was worked out by Pratt and Armi (1987). In order to make the problem analytically tractable, they examined a nonrotating flow with the linear potential vorticity distribution

$$q^*(\psi^*) = q_o^* - a\psi^*, \quad (2.9.8)$$

in a channel with rectangular cross section. Although $f=0$ this flow supports both gravity and potential vorticity waves and therefore contains the essential features we wish to investigate. Simplicity is provided by the fact that the d^* is uniform across the channel, $d^*=d^*(y^*)$ and that the expression for potential vorticity reduces to

$$q^* = \frac{\partial v^* / \partial x^*}{d^*} \quad (2.9.9).$$

Differentiation with respect to x^* and use of (2.9.8) leads to the cross-stream structure equation

$$\frac{\partial^2 v^*}{\partial x^{*2}} + ad^{*2} v^* = 0. \quad (2.9.10)$$

There are two distinct cases to consider. When $a < 0$, $dq^* / d\psi^* < 0$ and the potential vorticity has higher values on the right side of the channel (where $\psi^* = Q^*/2$) then on the left side (where $\psi^* = -Q^*/2$), although the variation of q^* across the channel may not be monotonic. As suggested in Figure 2.9.1a, this setting would seem to favor potential vorticity wave propagation in the same direction as the overall transport. In this case the solutions to (2.9.10) will be exponential. If $a > 0$ the situation is as shown in Figure 2.9.1b, with generally higher potential vorticity on the left and possible upstream propagation of potential vorticity waves. Here the solutions to (2.9.10) are oscillatory.

Consider the case $a < 0$ first. The solution to (2.9.10) can be written as

$$v^* = \frac{\hat{v}^* \sinh(\alpha x^*)}{\sinh(\frac{1}{2}\alpha w^*)} + \frac{\bar{v}^* \cosh(\alpha x^*)}{\cosh(\frac{1}{2}\alpha w^*)}, \quad (2.9.11)$$

where

$$\alpha(y^*) = |a|^{1/2} d^*(y^*),$$

$$\bar{v}^*(y^*) = \frac{1}{2}[v(\frac{1}{2}w^*, y^*) + v(-\frac{1}{2}w^*, y^*)],$$

and

$$\hat{v}^*(y^*) = \frac{1}{2}[v(\frac{1}{2}w^*, y^*) - v(-\frac{1}{2}w^*, y^*)].$$

As in Gill's (1977) model the flow has a boundary layer structure, each layer here having thickness α^{-1} . However there are some important differences. First, the decay scale depends only on the magnitude of the potential vorticity gradient $|\alpha| = |dq^* / d\psi^*|$

and the depth d^* , and not on gravity.¹ Furthermore, the decay scale *depends on the dependent variable* d and is therefore a function of y , whereas Gill's decay scale (L_d) was universally constant.

The boundary conditions $\psi^*(\pm \frac{1}{2}w^*) = \pm \frac{1}{2}Q^*$ may be used to relate \hat{v}^* , \bar{v}^* and d^* and form a hydraulic functional. The first step is to integrate the product of d^* and (2.9.11) across the channel, resulting in

$$\bar{v}^* = \frac{\alpha Q^* \coth(\frac{1}{2}\alpha w^*)}{2d^*}. \quad (2.9.12)$$

Next, the potential vorticity equation (2.9.9) is applied at $x^* = w^*/2$, leading to $\partial v^* / \partial x^* = d^*(q_o^* - \frac{1}{2}aQ^*)$. The use of (2.9.11) to evaluate $\partial v^* / \partial x^*$ there results in

¹ • The decay scale can also be written as $\left| \frac{v^*}{dq^* / dy^*} \right|^{1/2}$ which may be compared with the thickness

$\left(\frac{V}{\beta} \right)^{1/2}$ of inertial boundary currents on a beta-plane ocean. Here V is velocity scale and β is the planetary potential vorticity gradient.

$$\hat{v}^* = d^* q_o^* \alpha^{-1} \tanh(\frac{1}{2} \alpha w^*). \quad (2.9.13)$$

Finally a functional relation of the required form is obtained by evaluating the Bernoulli equation along the right-hand wall:

$$\frac{1}{2}(\bar{v}^* + \hat{v}^*)^2 + d^* + h^* = B_R^*. \quad (2.9.14)$$

Here B_R represents the right-wall value of the Bernoulli function. Substitution for \hat{v}^* and \bar{v}^* and nondimensionalization of the result leads to

$$\mathcal{G}(d; h, w) = \frac{1}{2} \left[\frac{1}{\tanh(\gamma d)} + \frac{\tanh(\gamma d)}{\Delta q} \right]^2 + d + h - B_R = 0 \quad (2.9.15)$$

where $(d, h, B_R) = (d^*/D, h^*/D, B_R^*/gD)$ and

$$\gamma = \frac{1}{2} w^* |a|^{1/2} D, \quad (2.9.16)$$

$$D = \frac{|a| Q^{*2}}{4g}, \quad (2.9.17)$$

and

$$\Delta q = \frac{|a| Q^*}{2q_o^*}, \quad (2.9.18)$$

all of which are non-negative.

$\mathcal{G}(d; h, w)$ contains two parameters γ and Δq . The former is one half the ratio of the channel width to the boundary layer thickness based on the scale depth D . It is a measure of the strength of potential vorticity effects over the cross-section of the flow. If $\gamma \ll 1$ potential vorticity effects are relatively weak. The other parameter Δq is a measure of the relative importance in the two terms q_o^* and $a\psi^*$ which comprise the potential vorticity. Specifically, Δq is the difference between the potential vorticity at the right and left walls normalized by their sum.

The critical condition $\partial \mathcal{G} / \partial d = 0$ leads to

$$\gamma \sinh(\gamma d_c) \operatorname{sech}^3(\gamma d_c) [\coth^4(\gamma d_c) - \Delta q^{-2}] = 1 \quad (2.9.19)$$

and the left-hand side of this expression decreases monotonically from positive ∞ to zero, indicating at most a single root. Figure 2.9.2 shows an example of a solution curve (2.19.15) with B_R-h plotted as a function of d with $\Delta q = 1$ $\gamma = 1$ (the constant implying that the channel width is uniform). Solutions are constructed in the usual way by following the curve as h changes, with a hydraulic transition if the maximum h occurs at

the minimum of the curve. Furthermore, it may be shown that in the limit of vanishing Δq and γ that (2.9.19) reduces to the result for one-dimensional flow: $\bar{v}^* = v^* = (gd^*)^{1/2}$. In this limit the left- and right-hand branches of the solution curves correspond respectively to supercritical and subcritical flows. We will assume that this characterization continues to hold for non-zero Δq and γ with the caveat that the actual wave speeds along the two branches have not been calculated.

There is nothing so far that dramatically distinguishes the character of the model from its one-dimensional counterpart. However, a closer look at the velocity structure reveals an important differences, namely that stagnation points with corresponding separating streamlines can exist on the left-hand wall. The required condition is $\hat{v}^* = \bar{v}^*$, or if (2.9.12) and (2.9.13) are used:

$$\Delta q = \tanh^2(\gamma d_s). \quad (2.9.20)$$

Here d_s denotes the value of d at the section of wall stagnation. The corresponding right-wall condition is obtained by reversing the sign of the right-hand term and cannot be satisfied for positive Δq . Hence, stagnation can occur only on the left wall. The use of (2.9.20) to substitute for Δq in the critical condition, (2.9.19) leads to

$$\gamma \frac{\sinh(\gamma d_c)}{\cosh^3(\gamma d_c)} [\coth^4(\gamma d_c) - \coth^4(\gamma d_s)] = 1, \quad (2.9.21)$$

and thus d_c must be $< d_s$ (the flow must be subcritical) for separation to occur. This *stagnation* separation should be distinguished from the rotation induced separation in which the wall depth vanishes. In Figure 2.9.2, subcritical solutions with $d > d_s$ are indicated by dashing. In this case, most of the subcritical curve has this property. Corresponding velocity profiles will have reverse flow along the left-hand wall. Figure 2.9.3 shows an example of the velocity upstream, downstream of, and at the controlling sill. The three sections correspond to points A, B, and C of the solution curve. Immediately upstream of the sill lies the stagnation point and beyond it a counterflow. At section A most of the channel contains recirculating fluid; only that passing close to the right wall reaches the sill.

We now turn to the more interesting case $a > 0$, which is favorable for potential vorticity wave propagation against the mean flow. The solution to (2.9.10) is

$$v^* = \hat{v}^* \frac{\sin(\alpha x^*)}{\sin(\alpha w^*/2)} + \bar{v}^* \frac{\cos(\alpha x^*)}{\cos(\alpha w^*/2)}, \quad (2.9.22)$$

so that the velocity profile is oscillatory. Repeating the above procedure leads to

$$\bar{v}^* = \frac{\alpha Q^* \cot(\alpha w^*/2)}{2d^*} \quad (2.9.23)$$

and

$$\hat{v}^* = \frac{q_o^* d^* \tan(\alpha w^* / 2)}{\alpha}. \quad (2.9.24)$$

Substitution of (2.9.23) and (2.9.24) into the Bernoulli equation (2.9.14) and nondimensionalization gives

$$\mathcal{G}(d; h, w) = \frac{1}{2} \left[\cot(\gamma d) + \frac{\tan(\gamma d)}{\Delta q} \right]^2 + d + h - B_R = 0 \quad (2.9.25)$$

where γ and Δq are defined as before and are considered positive. Note that the squared term is has the value $+\infty$ for $\gamma d = \frac{1}{2} n\pi$ ($n = 0, 1, 2, \dots$), suggesting that the solution ‘curve’ consists of a series of disconnected lobes. This is confirmed by a plot (Figure 2.9.4) showing $B_R - h$ as a function of d for $\gamma = \Delta q = 1$. Each lobe is numbered from left to right and the minimum value $B_R - h$ increases as the lobe number increases. For a given upstream state (here determined by B_R) and a given topographic elevation h , there may be more than two possible steady states. For example the value $B_R - h = 10$ corresponds to 12 possible states. However, once a particular solution lobe is determined (say by upstream conditions), then at most two states are possible for any given h . Of course, a hydraulic jump or some other nonconservative feature might allow the solution to jump from one lobe to another, thereby allowing more possibilities.

Stagnation along the left wall is also possible and occurs when $\hat{v}^* = \bar{v}^*$, or

$$\Delta q = \tan^2(\gamma d_s). \quad (2.9.26)$$

As before, separation along the right wall is not possible for non-zero Δq .

At the minimum of each lobe the flow is critical and the corresponding depth d_c can be calculated from the condition $\partial \mathcal{G} / \partial d = 0$, which yields

$$\gamma \frac{\sin(\gamma d_c)}{\cos^3(\gamma d_c)} [\cot^4(\gamma d_c) - \cot^4(\gamma d_s)] = 1. \quad (2.9.27)$$

It can be shown using (2.9.6) and (2.9.7) that $d_s > d_c$ within each lobe.

The most obvious qualitative difference between solutions corresponding to different lobes is in the number of zero crossings of the cross-channel profile of v . It can be shown that the solutions corresponding to lobe n have either n or $n-1$ zero crossings, the greater number occurring for larger values of d . Thus the higher lobes correspond to intricate flows with multiple bands of fluid moving upstream and downstream. Figures 2.9.5a and 2.9.5b show examples taken from lobes #1 and #2.

There remains some mystery concerning solutions corresponding to different solution lobes. If the cross-channel reduced by taking the limits γ and $\Delta q \rightarrow 0$, lobe #1 tends toward the solution curve for a one-dimensional, nonrotating flow (e.g. Figure 1.4.1). The inset of Figure 2.9.4 shows how this limit is approached; as γ and Δq are reduced; the depth range of the first lobe grows and the remaining lobes are pushed off to infinity. Controlled solutions belonging to the first lobe appear then to be governed by the dynamics of a shear-modified, long gravity wave. For the other solutions, it is evident that the relative change in depth across the sill relatively small and becomes vanishingly so for the higher lobes. The change in the flow as it passes through a critical section occurs primarily one of horizontal structure. This idea can be formalized by calculating the cross sectional enstrophy

$$E_n^* = \frac{1}{2} \int_{-w^*/2}^{w^*/w} (\partial v^* / \partial x^*)^2 dx = \frac{1}{2} d^{*2} \int_{-w^*/2}^{w^*/w} q^{*2} dx, \quad (2.9.28)$$

a measure of the horizontal shear across a particular section. As explored in Exercise 3 it can be shown that the change in E_n^* caused by a small change in depth as the flow passes through a critical section increases as the lobe number becomes higher. This indicates that control of the flow by the higher lobes primarily affects the horizontal shear and not the depth. Because of this feature, and because the higher lobes owe their presence entirely to a finite potential vorticity gradient, it is evident that the corresponding solutions are controlled by a potential vorticity wave.

Further to the ongoing discussion, it can be shown that Stern's condition for criticality (2.9.6) succeeds in predicting the control condition for the first lobe, but fails for the remaining lobes. Failure is due to the fact that the higher lobe solutions all have velocity reversals, whereas the derivation of (2.9.6) assumes unidirectional flow. Flows with potential vorticity gradients may therefore experience a multiplicity of controlled configurations, not all of which obey Stern's criterion.

A final consideration, one that could render much of the above discussion academic, is stability. The most pertinent theorem for the present case is Fjortoft's necessary condition for instability (see Drazin and Reid, 1981), which does not strictly apply to our flow in general, but would be applicable if the flow was bounded by a rigid lid. Instability is possible when $dq^*/d\psi^* < 0$, or $a > 0$, the case permitting multiple solutions.

There remains uncertainty regarding the interpretation of the $a > 0$ solutions, how they are established, which branches of the higher lobes are supercritical and subcritical, and what their stability is. One of the difficulties is that the model contains a mix of potential vorticity and gravity wave dynamics. More recent investigations of hydraulic effects in presence of potential vorticity gradients have utilized models that expunge gravity waves by placing a rigid lid on the surface. Also, piecewise constant (rather than continuous) distributions of q^* can reduce the number of waves modes to just one or two,

further simplifying the problem and allowing the peculiar dynamics to be investigated in isolation. These models take us away from the topics and applications of the current chapter but they are revisited in Chapter 6.

Exercises

- 1) Obtain the result (2.9.6) starting with the trivial relation

$$w = \int_{-w/2}^{w/2} dx$$

and change the integration variable x to ψ . (What does this the use of this last tranformation assume about the flow?). Attempt to cast the new integral as a Gill type functional in a single variable and use the result to obtain a critical condition.

- 2) Use the manipulations from the following text to construct a homework problem in which one obtains Stern's result. This is basically going from the second equation before 2.9.6 to the first eq. before 2.9.6.

Application of Leibnitz's rule to the derivative of I .

$$\text{Let } I = \int_{f_1(d_o)}^{f_2(d_o)} \frac{\partial I}{v_{\pm}(d, d_o)} \text{ with } v_{\pm} \text{ defined by (10). Then}$$

$$\frac{\partial I}{\partial d_o} = \frac{f_2'}{v_{\pm}(f_2, d_o)} - \frac{f_1'}{v_{\pm}(f_1, d_o)} + \int_{f_1}^{f_2} \frac{\partial}{\partial d_o} \frac{1}{v_{\pm}} \partial d \quad (\text{A1})$$

The above result if valid for all values of d_o in an interval $a < d_o < b$ provided that v_{\pm}^{-1} and $\partial v_{\pm}^{-1} / \partial d_o$ are continuous in $f_1 \leq d \leq f_2$ and $a < d_o < b$, and also that f_1' and f_2' are continuous in $a < d_o < b$. (Hildebrand, p. 365). Clearly v_{\pm} cannot go to zero in the interval $f_1 \leq d \leq f_2$.

Now, from (10)

$$\frac{\partial v_{\pm}^{-1}}{\partial d_o} = \frac{d_o B'}{v_{\pm}^3}$$

and

$$\frac{\partial v_{\pm}^{-1}}{\partial d} = \frac{1 - d B'}{v_{\pm}^3}$$

so that

$$\frac{\partial v_{\pm}^{-1}}{\partial d_o} = \frac{d_o}{d} \left(\frac{1}{v_{\pm}^3} - \frac{\partial v_{\pm}^{-1}}{\partial d} \right)$$

Substitution into (A1) gives

$$\frac{\partial I}{\partial d_o} = \frac{f_2'}{v_{\pm}(f_2, d_o)} - \frac{f_1'}{v_{\pm}(f_1, d_o)} + \int_{f_1}^{f_2} \frac{d_o}{d} \left(\frac{1}{v_{\pm}^3} - \frac{\partial v_{\pm}^{-1}}{\partial d} \right) \partial d$$

Integrating the last term by parts gives

$$\frac{\partial I}{\partial d_o} = \frac{f_2'}{v_{\pm}(f_2, d_o)} - \frac{f_1'}{v_{\pm}(f_1, d_o)} - d_o \left(\frac{1}{f_2 v_{\pm}(f_2, d_o)} - \frac{1}{f_1 v_{\pm}(f_1, d_o)} \right) + d_o \int_{f_1}^{f_2} \left(\frac{1}{dv_{\pm}^3} - \frac{1}{d^2 v_{\pm}} \right) \partial d \quad (\text{A2})$$

3) Show that the velocity profile (2.9.22) can be written in the nondimensional form

$$v = \frac{\sin(\gamma dx)}{\Delta q \sin(\gamma d)} + \frac{\cos(\gamma dx)}{\cos(\gamma d)},$$

where $v = 2v^* / |a|^{1/2} q$, $d = d^*/D$, $x^* = x/(w^*/2)$ and γ is as defined above. Using this expression, calculate the nondimensional version E_n of the enstrophy E_n^* (first equality in 2.9.28). Now take derivative of the result with respect to d and evaluate at the critical depth. From the result, show that

$$(\partial E_n / \partial d)_{d=d_c} \sim d_c^2 \quad (d_c \rightarrow \infty),$$

and therefore the change in enstrophy relative to a change in depth increases as the critical depth (and therefore the lobe number) increases.

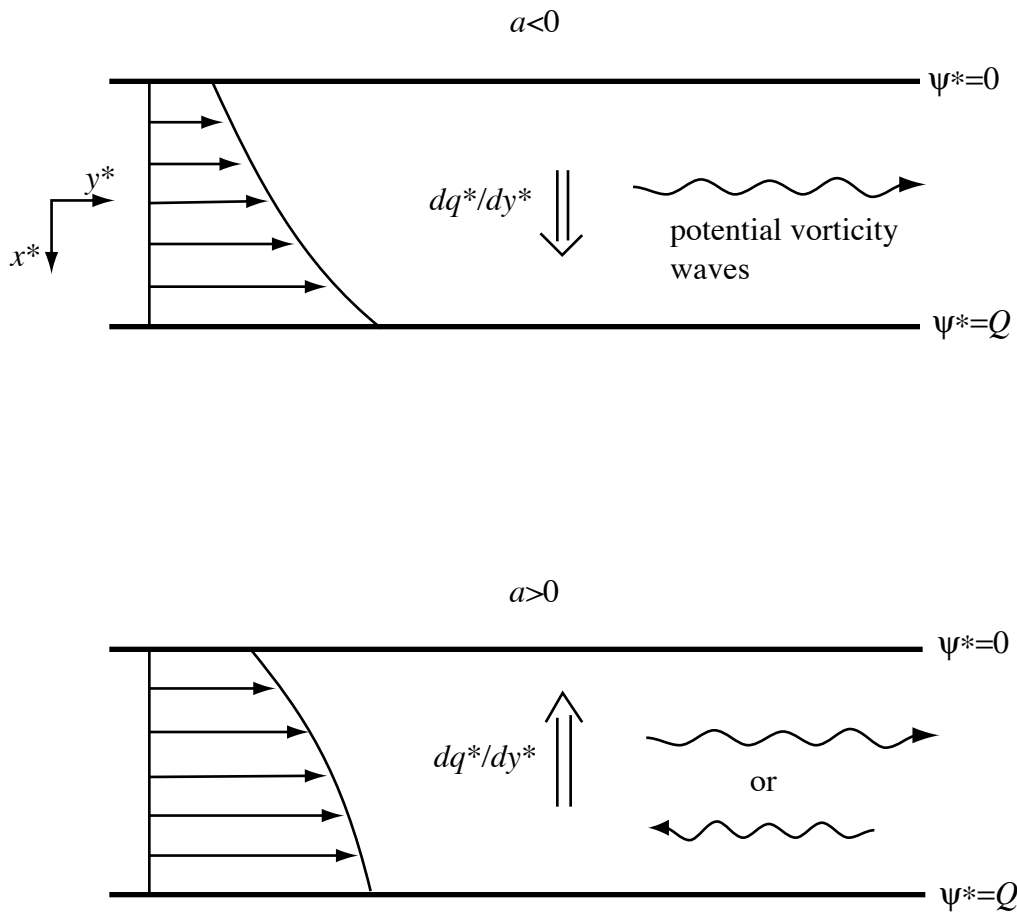


Figure 2.9.1

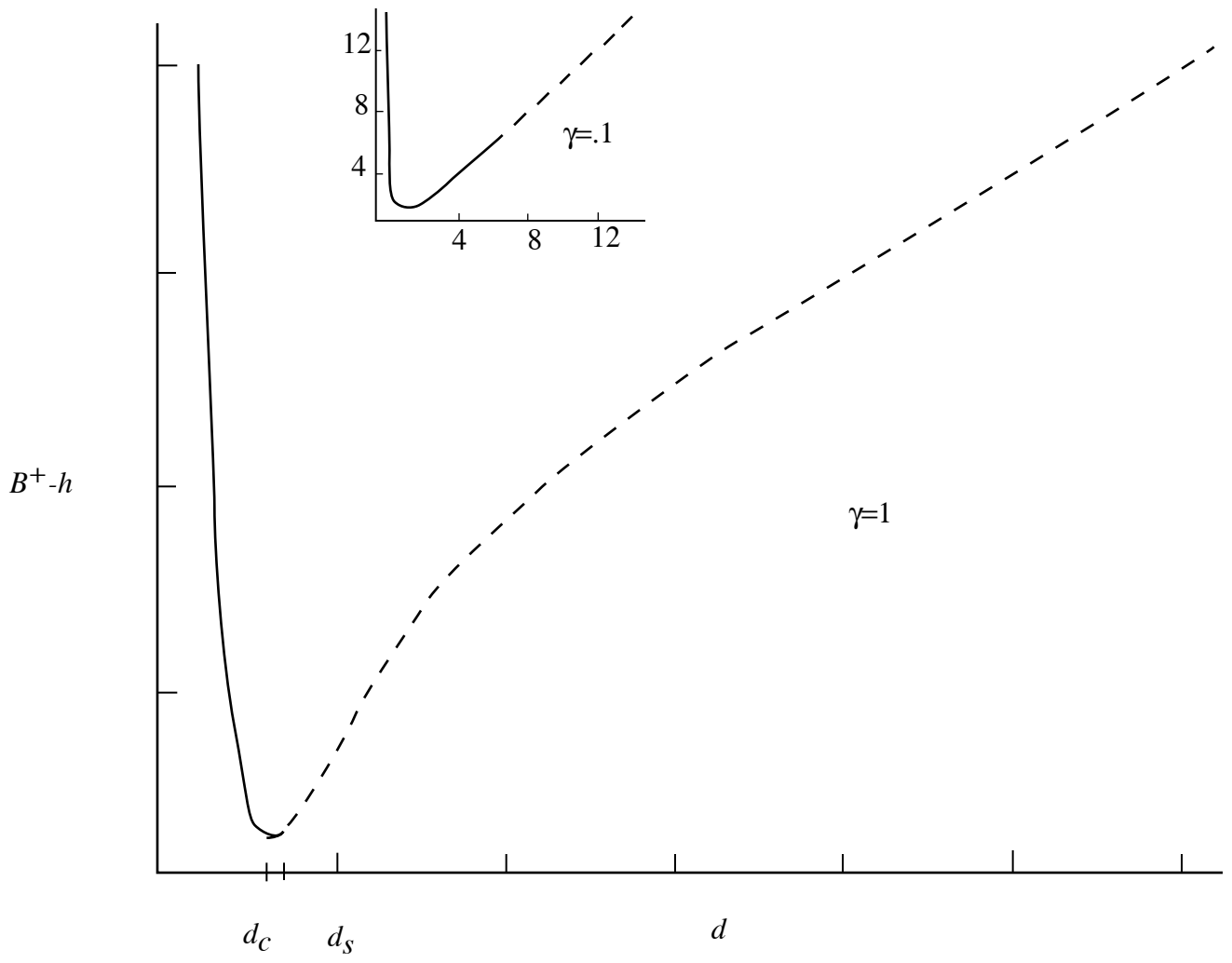


Figure 2.9.2

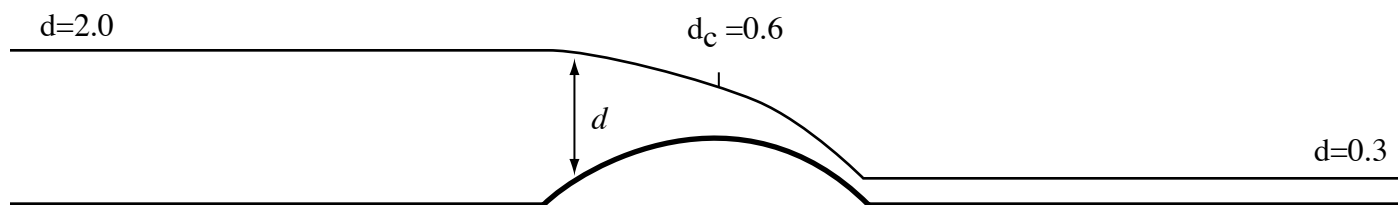
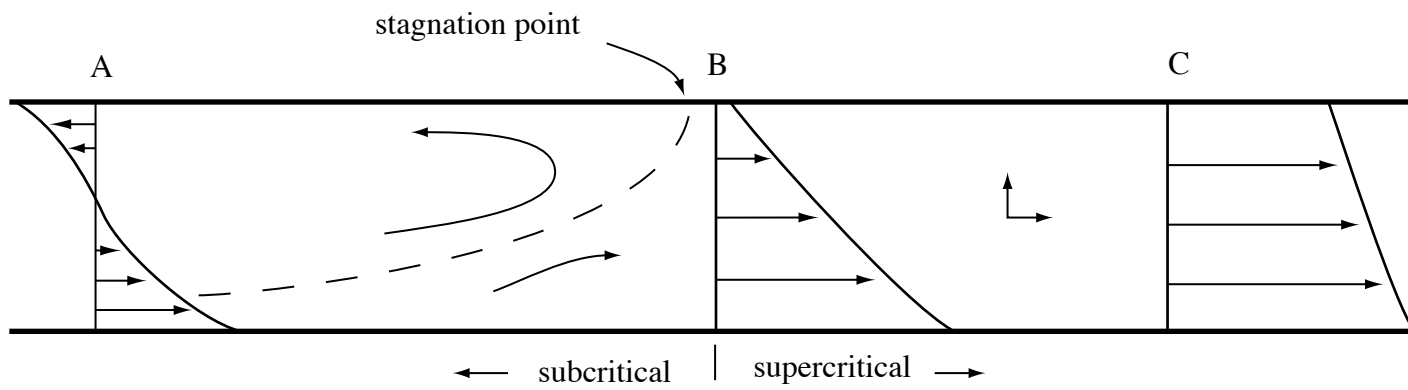


Figure 2.9.3

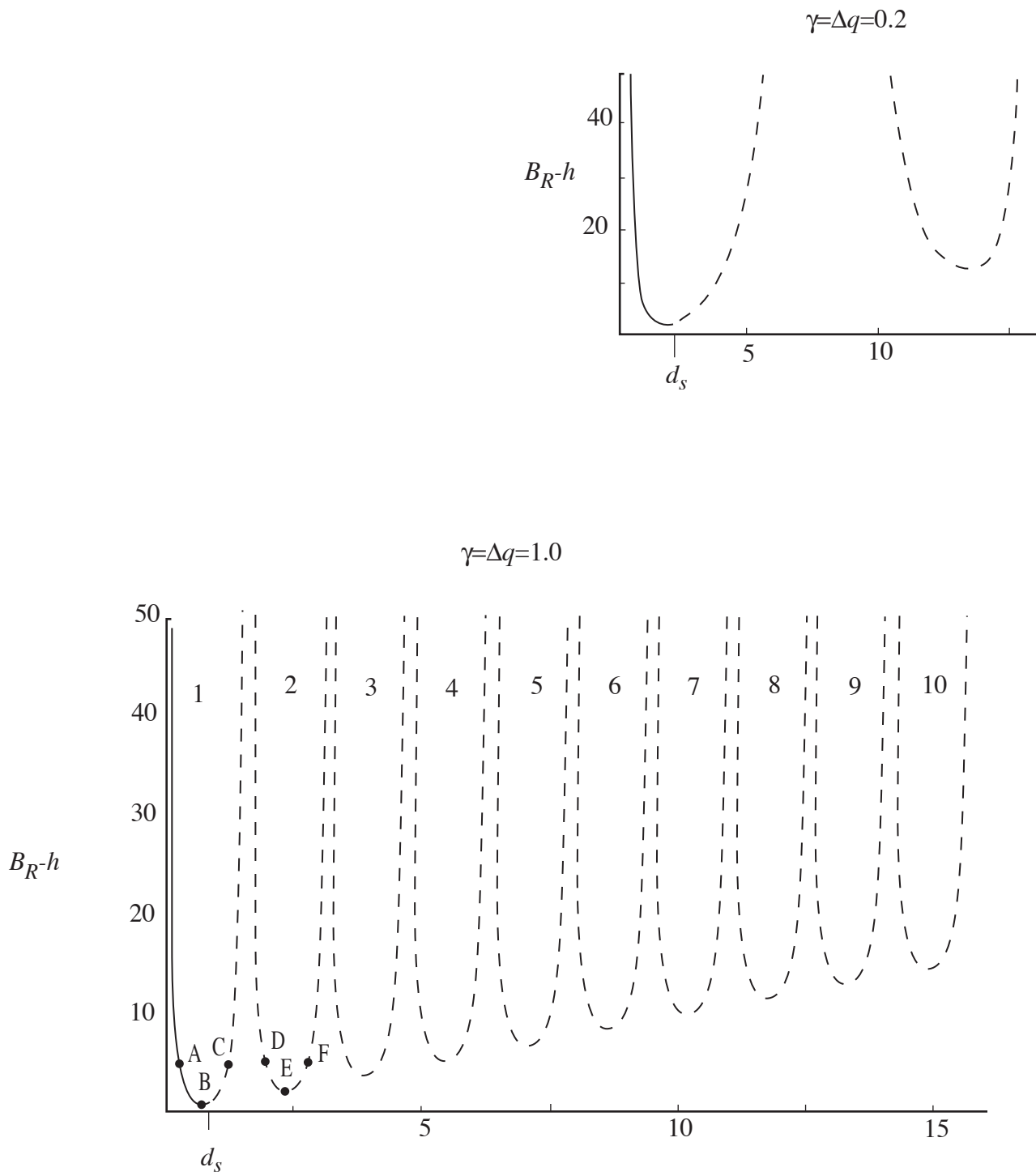


Figure 2.9.4

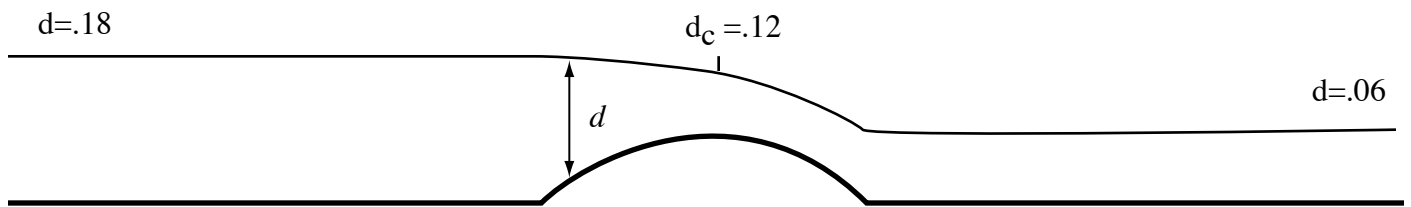
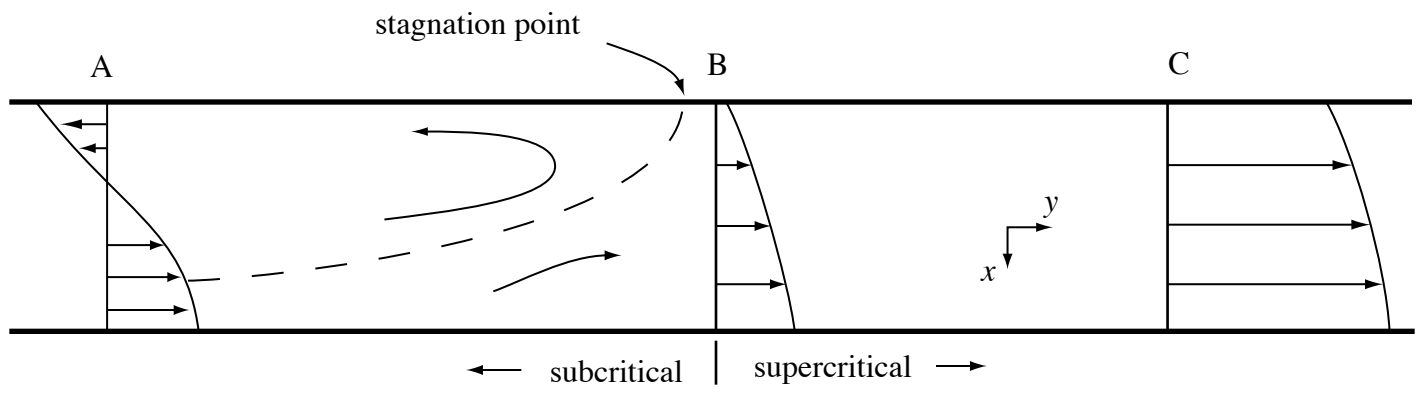


Figure 2.9.5

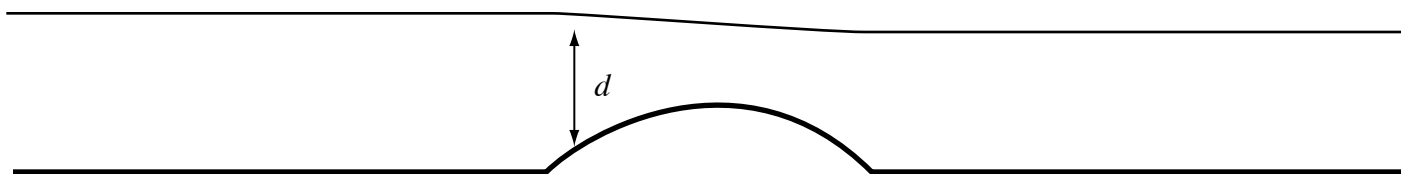
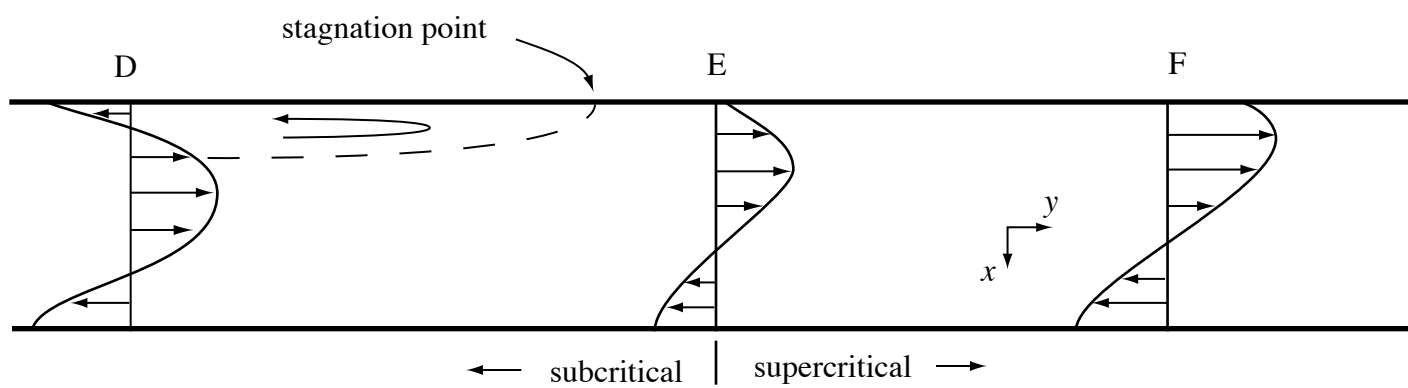


Figure 2.9.6